ON THE RELATIONSHIP BETWEEN THE EARTH'S WEAK STABILITY BOUNDARY REGION AND THE LOW-ENERGY TRANSFERS TO THE MOON

Elena Fantino [1,2], Gerard Gómez [1,3], Josep J. Masdemont [1,2], Yuan Ren [1,2]

[1] *Institut d'Estudis Espacials de Catalunya, Gran Capità 2-4, 08034 Barcelona, Spain*

[2] *Departament de Matemàtica Aplicada I, ETSEIB, Universitat Politècnica de Catalunya, Diagonal 647, 08028 Barcelona, Spain, +34 93406550, elena.fantino@upc.edu, josep@barquins.upc.edu, yuan.ren@upc.edu*

[3] *Departament de Matemàtica Aplicada i Anàlisi, Universitat de Barcelona, Gran Via 585, 08007 Barcelona, Spain, +34 934021651, gerard@maia.ub.es*

ABSTRACT

The term Weak Stability Boundary (WSB) is related to a region of stable motion around the second primary of a circular restricted three-body problem (CR3BP). Previous work on this subject has shown that, at a given energy level, the boundaries of such region are provided by the stable manifolds of central objects of the L_1 and L_2 libration points, i.e., the two planar Lyapunov orbits (PLOs). This offers a natural dynamical channel between the Earth's vicinity and the Sun-Earth libration points L_1 and L_2. Furthermore, it has been shown (and successfully employed to design low-energy spacecraft lunar transfers) that the Sun-Earth L_2 central unstable manifolds can be linked, through an heteroclinic connection, to the central stable manifolds of the L_2 point in the Earth-Moon three-body problem. The aim of the present study is to clarify the relationship between the low-energy Earth-to-Moon transfers (LETs) and the dynamics of the phase space points that populate the WSB region around the Earth. The present work develops through an extensive and systematic exploration of the trajectories connecting planar Lyapunov orbits corresponding to all the possible combinations of two libration points in the Sun-Earth and Earth-Moon CR3BPs, kinematically coupled. The results of such exploration give us a deeper and more complete understanding of the dynamics and properties of such connections and constitute the basis for the next stage of the investigation, that is the study of the structure of the WSB around the Earth, its dynamical relationship first with the Sun-Earth libration points L_1 and L_2 and then with the Earth-Moon ones, in the bicircular four-body model. This investigation is part of a research work that will be the subject of a subsequent, more extended publication.

KEYWORDS – three-body problem, four-body problem, libration points, periodic orbits, invariant manifolds, numerical integration.

1. INTRODUCTION

The LETs consist in connecting trajectories belonging to the invariant manifolds of the central objects around the collinear libration points L_1 and L_2 of the Sun-Earth and Earth-Moon CR3BPs in such a way as to almost naturally reach the Moon's vicinity from a low-Earth orbit. The mechanism that explains the LETs was first presented in [5]. Fig. 1 illustrates the idea for the planar case in the Sun-Earth barycentric synodical reference frame: a branch of a stable manifold of a planar Lyapunov orbit around L^{SE}_2 (i.e., the Sun-Earth L_2 point) drives the spacecraft away from the Earth, then the unstable manifold

of the same PLO redirects it to a region where also the stable manifold of a PLO of the L^{EM}_2 (i.e., the Earth-Moon L_2 point) point flows. There, the intersection in configuration space (trough a conveniently set Poincaré section) is sought. The difference in velocity between the two intersecting trajectories (which may be equal to zero if there is a heteroclinic connection) constitutes the cost of the transfer. The dynamical characteristics of the two CR3BPs and their kinematical relationship are such that low-cost (and even zero cost) connections of the type L^{EM}_2 -L^{SE}_2 can easily be found.

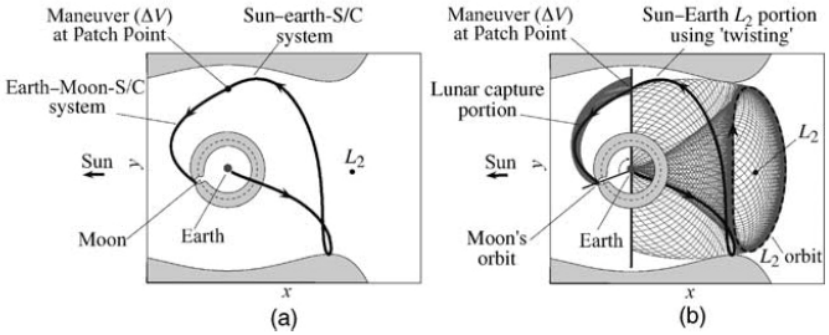

Fig. 1. A low-energy transfer from the Earth to the Moon through the L_2 Lagrange points of the SE and EM systems as seen in the SE synodical barycentric reference frame (a) and its construction based on patching invariant manifolds of the SE and EM CR3BPs (b) ([5]).

The concept of WSB was first introduced by [6] in connection with the rescue of the lunar spacecraft Hiten. As shown by [5], the rescue was possible due to the combined gravitational influences of the Earth, the Moon, and the Sun. Although the WSB region has not an analytic definition, there is an algorithmic one (see [1] and [4]) which distinguishes between stable and unstable points according to the dynamical evolution of initial two-body orbits around the second primary when the first primary is introduced: its gravitational influence may be such that the third body cannot complete one (or more) full revolution around the second primary without changing the sign of its total mechanical two-body energy or without first performing a full revolution around the first primary. When this is the case, the given initial condition is said to be unstable. More on the WSB regions in the Sun-Earth-Moon system can be found in [3] and [8], also in connection with the design of Earth-to-Moon trajectories.

The aim of the present study is to unify the concepts of LET and WSB, or equivalently to show that the WSB points that reach the Moon's vicinity are driven by the stable and unstable invariant manifolds of the two CR3BPs and are responsible for performing the heteroclinic connections between libration point orbits that constitute the framework of the low-energy transfers from the Earth to the Moon.

The present study starts with the study of all the L^{EM}_i -L^{SE}_j (i,j=1,2) connections between the Earth-Moon and the Sun-Earth systems: it consists in a full, systematic exploration of such transfers in the framework of a two-coupled CR3BPs, aiming at identifying the conditions under which zero-cost and low-cost connections are possible (Section 2). As a whole, these explorations form what we call the L^{SE}_i-L^{EM}_j connections. This will be followed by the characterization of the WSB regions of the Earth and the Moon in the framework of the CR3BP and their relationship with the invariant manifolds of the

PLOs around L_1 and L_2 will be outlined (Section 3). Section 4 connects the two issues by following the motion of the unstable points of the Earth's WSB at a given energy level through capture at L^{SE}_1 or L^{SE}_2 and until the Moon and its libration points are approached. This is accomplished from within the Bicircular Four-Body Problem (B4BP), in which the gravitational influence of all three primaries (i.e., Sun, Earth and Moon) is simultaneously taken into account. Section 5 concludes and illustrates the current stage and future developments of the present work.

2. L^{SE}_i-L^{EM}_j CONNECTIONS

Following [5], the connections are computed in the framework of the coupled CR3BP in which the Sun-Earth (SE) and the Earth-Moon (EM) three-body problems are kinematically linked in inertial space through their orbital initial phases α^{SE}_0 and α^{EM}_0, respectively. Two are the critical parameters, i.e., the choice of the Poincaré section (PS) and the value of the initial ($t=0$) relative orbital phase $\alpha_0 = \alpha^{EM}_0 - \alpha^{SE}_0$ between the two CR3BPs. The PSs adopted in this study are two-dimensional planes of the type $x = x_p$, where x_p is an appropriately chosen value of the x coordinate in the SE CRTBP frame of reference, and the two dimensions of the plane are along y and v_y. All computations concerning quantities pertaining to the SE problem are made in such reference frame, whereas those pertaining to the EM problem are carried out in the EM CR3BP frame of reference and then transformed into the other. The intersections of the manifolds with the given PS are approximated numerically by means of some iterative procedure like the bisection or Newton methods. As a result, each manifold generates one (closed) curve on the PS. If the two curves intersect (and under normal conditions this occurs in two points) a connection in configuration space (xy) is said to exist between the two given LPOs, i.e., it is possible to compute two pairs of trajectories that perform the connection through the two given intersection points. In velocity space, the v_y components of the connecting trajectories are equal by construction, whereas in general $\mathrm{v}_x^{\mathrm{EM}} \neq \mathrm{v}_x^{\mathrm{SE}}$. Their difference defines the cost $\Delta \mathrm{v}$ of the given connection. Note that $\mathrm{v}_x^{\mathrm{EM}}$ and $\mathrm{v}_x^{\mathrm{SE}}$ are computed in the frame of reference of each CR3BP from the remaining components of the corresponding state vector, from the value of the Jacobi constant J and exploiting the definition of the latter, i.e.:

$$v_x = \pm\left[x^2 + y^2 + \frac{2(1-\mu)}{r_1} + \frac{2\mu}{r_2} + \mu(1-\mu) - \dot{y} - J \right]^{1/2} \tag{1}$$

μ is the mass ratio of the given RTBP (SE or EM), r_1 and r_2 are the distances of the third body from the first and the second primary, respectively. Of the two ΔV 's found, the lower is selected.

2.1 Simulations

Starting from a database of initial conditions for 70 planar Lyapunov orbits in the SE CR3BP and 70 planar Lyapunov orbits in the EM CR3BP around each of the two collinear Lagrange points L_1 and L_2, all the possible pairs of such orbits, one for each system, have been formed and the invariant manifold transfers of the kind described above have been sought for each such combination. The range of energy levels covered (expressed in terms Jacobi constant values) is [3.10, 3.20] for the Earth-Moon system and [3.00058,3.00090] for the Sun-Earth system. 72 values of the initial relative orbital phase α_0 (i.e.,

$0^o \le \alpha_0 \le 360^o$ at steps $\Delta\alpha_0 = 5^o$) between the two CR3BP problems have been considered. Six PS positions have been considered at $x = x_p$ (p=1,6) on the x-axis of the SE CR3BP frame of reference,

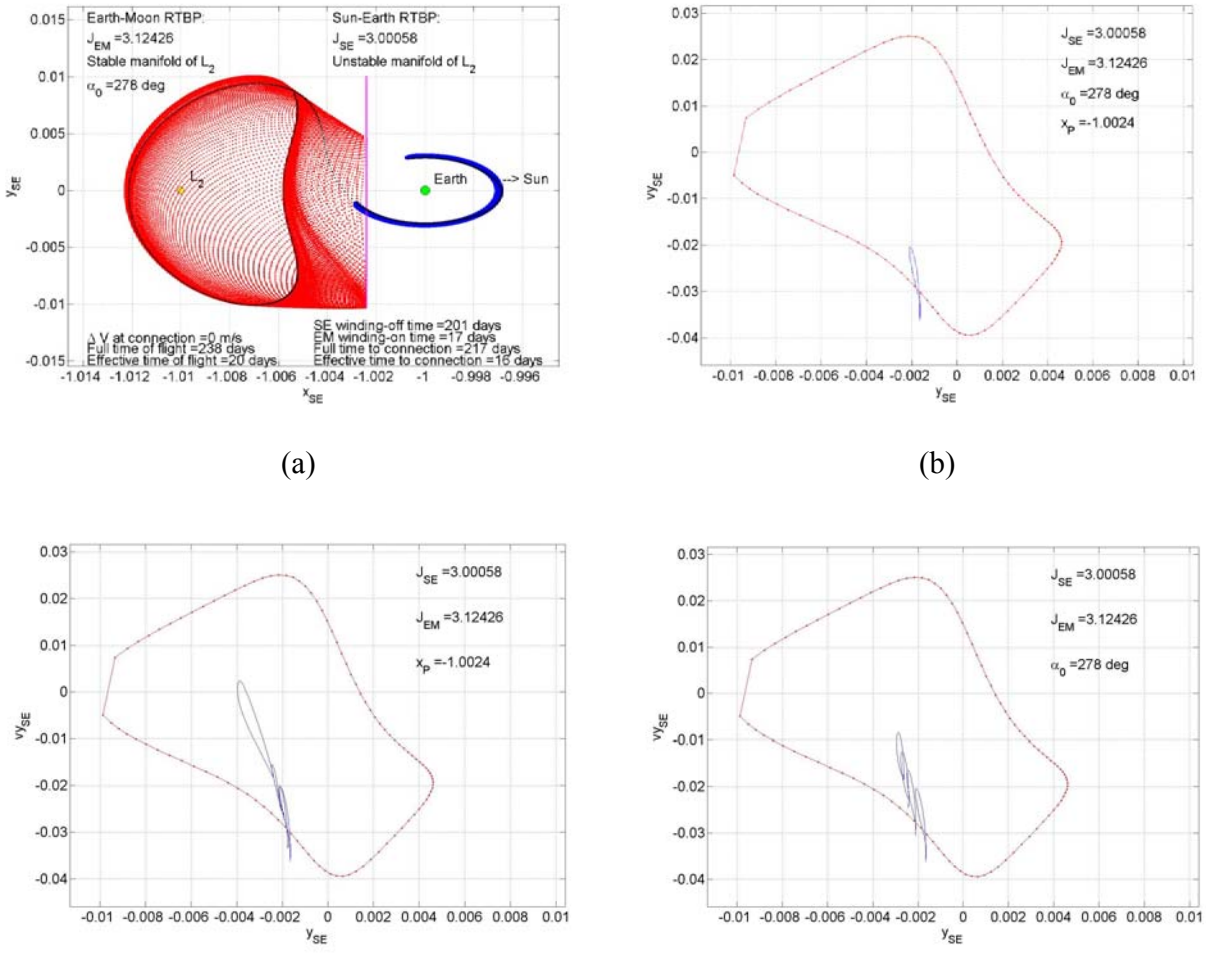

Fig. 2. Example of a low-cost connection of the type L^{SE}_2 - L^{EM}_2: view of the LPOs, their manifolds and the connecting trajectory in configuration space (SE synodical barycentric coordinates) (a), the intersection on the Poincaré section (b), the intersections on the PS when the initial relative orbital phase between the two systems is made to vary (c), the intersections on the PS when the x-coordinate of the PS is made to vary (d).

placed between the Earth and the given SE PLO. The numerical integration has been performed with a Runge-Kutta 7-8 method. The time required to accomplish a full transfer from a given SE PLO to a given EM PLO has been approximated with the difference between the time of flight on each trajectory and the time required to wind off/on the corresponding periodic orbit (until a distance to the orbit equal to 10^{-3} dimensionless units is reached).

Here below we present examples of individual connections for each L^{SE}_i-L^{EM}_j combination and global results for each type. Figs. 2, 3, 4 and 5 illustrate cases of low- or zero-cost connections: in particular,

the connection in the SE RTBP reference frame with the PLOs and their manifolds, the Jacobi constant values in the two problems, the time of flight and initial relative orbital phase are given. Then the view of the intersection of the two manifolds on the PS is provided. Figs. 6, 7, 8 and 9 are colour maps (respectively in 3D on the left and 2D on the right) of the cost required to transfer between specified energy levels (indicated respectively on the *x*- and *y*-axes of the plots for the SE and EM systems). The darkest areas represent the lowest-cost connections.

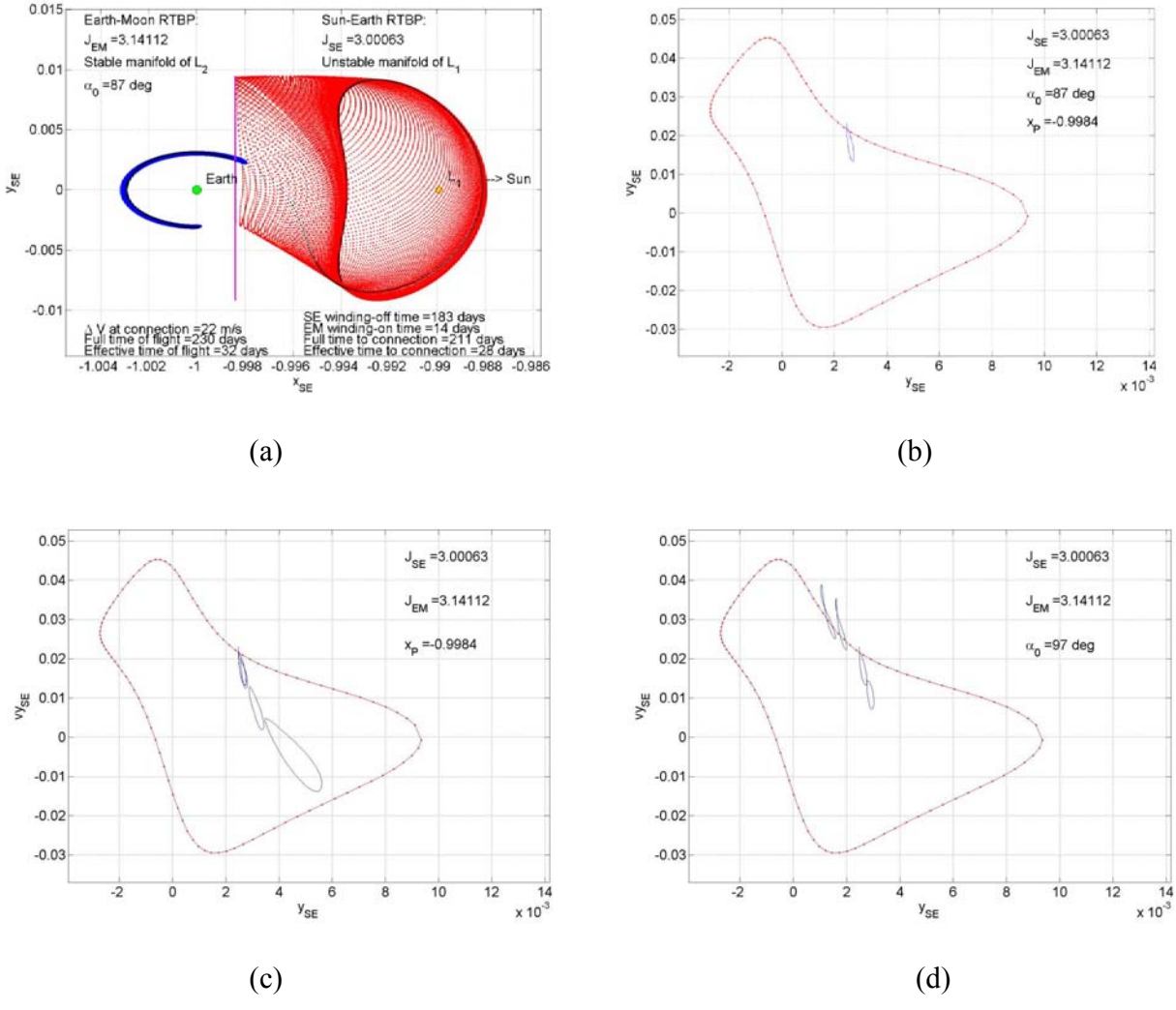

Fig. 3. Example of a low-cost connection of the type L^{SE}_1 - L^{EM}_2: view of the LPOs, their manifolds and the connecting trajectory in configuration space (SE synodical barycentric coordinates) (a), the intersection on the Poincaré section (b), the intersections on the PS when the initial relative orbital phase between the two systems is made to vary (c), the intersections on the PS when the *x*-coordinate of the PS is made to vary (d).

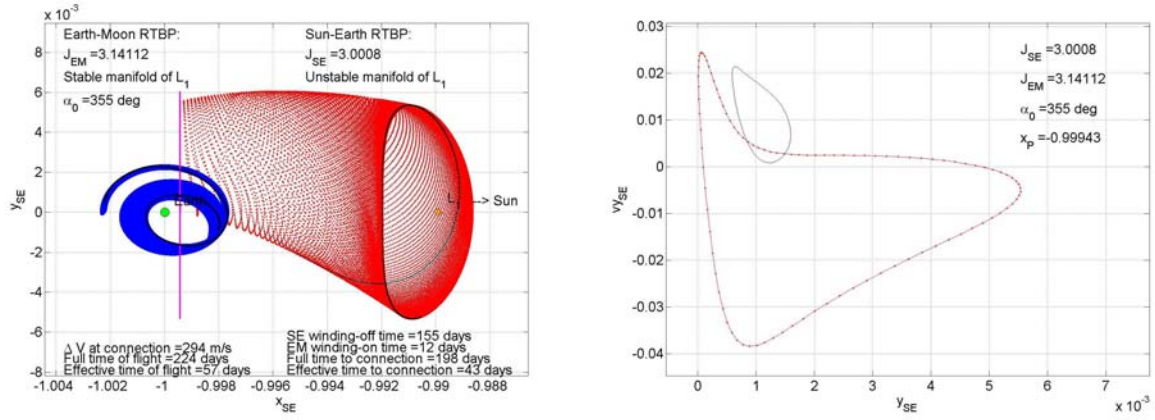

Fig. 4. Example of a connection of the type L^{SE}_1 - L^{EM}_1: view of the LPOs, their manifolds and the connecting trajectory in configuration space (SE synodical barycentric coordinates) (left) and the intersection on the Poincaré section (right).

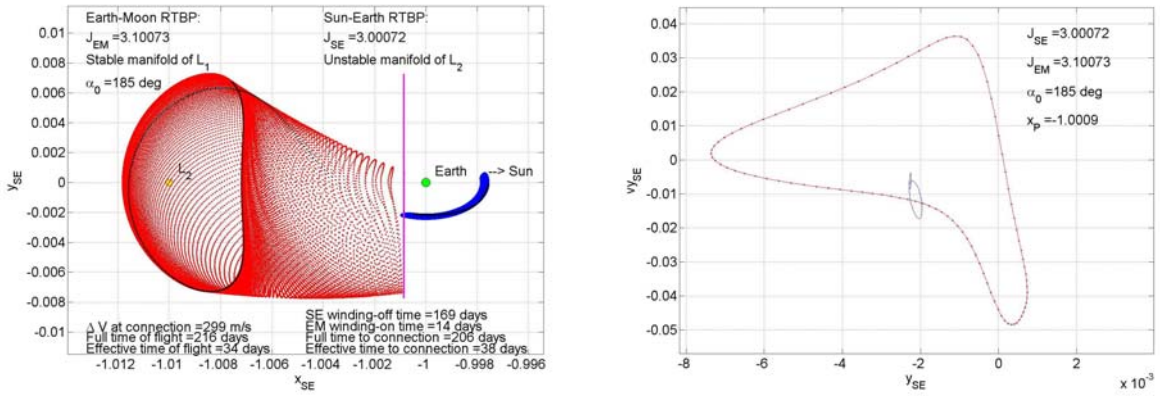

Fig. 5. Example of a connection of the type L^{SE}_2 - L^{EM}_1: view of the LPOs, their manifolds and the connecting trajectory in configuration space (SE synodical barycentric coordinates) (left) and the intersection on the Poincaré section (right).

Inspection of Figs. 6 and 7 shows that the combinations L^{SE}_2 - L^{EM}_2 and L^{SE}_1 - L^{EM}_2 provide heteroclinic connections (i.e, zero-cost transfers) over a large range of energy values. In the remaining two cases, i.e., L^{SE}_2 - L^{EM}_1 and L^{SE}_1 - L^{EM}_1 (Figs. 8 and 9) this is no longer true. To obtain a connection between the manifolds of those Lyapunov orbits, a minimum ΔV at the Poincaré section of at least 250 *m/s* is required. Our investigations suggest that the reason for this resides in the much higher velocities that characterize the Earth-Moon invariant manifolds associated to periodic orbits around the libration point L^{EM}_1 after transformation into the Sun-Earth barycentric synodical reference frame, with respect to the values found for the invariant manifolds associated to L^{EM}_2: the latter, not only intersect the Sun-Earth invariant manifolds in configuration coordinates, but also in velocity space, thus producing a wide number of heteroclinic connections.

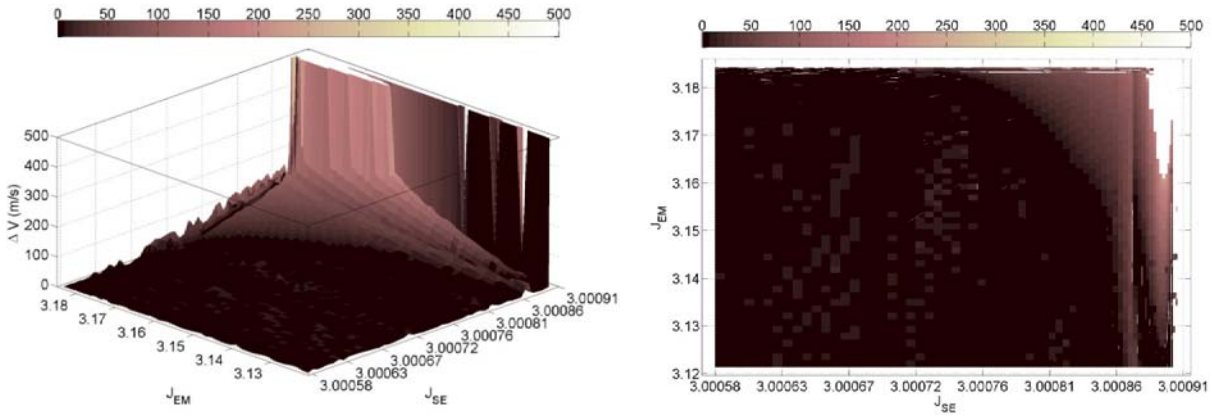

Fig. 6. 3D (left) and 2D (right) color maps of minimum ΔV for connections of type L^{SE}_2 - L^{EM}_2 as a function of the Jacobi constant of the two systems.

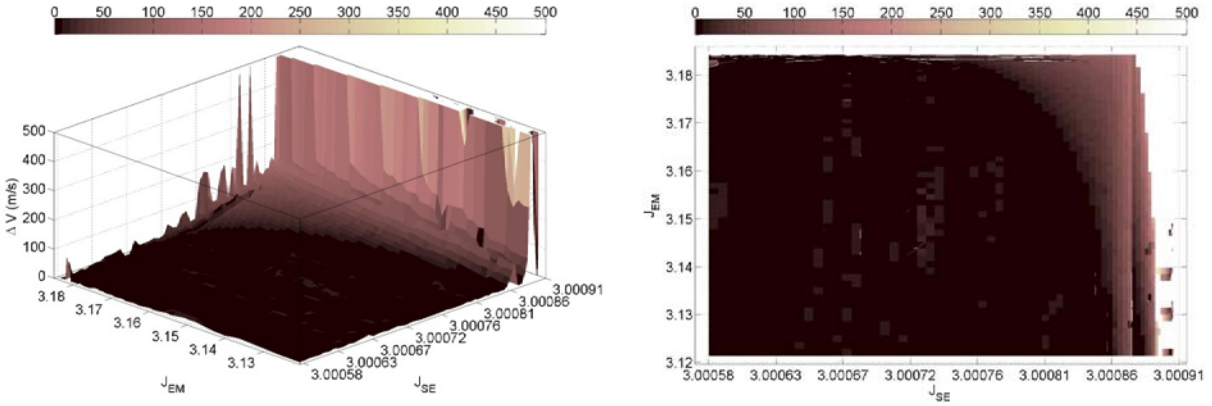

Fig. 7. 3D (left) and 2D (right) color maps of minimum ΔV for connections of type L^{SE}_1 - L^{EM}_2 as a function of the Jacobi constant of the two systems.

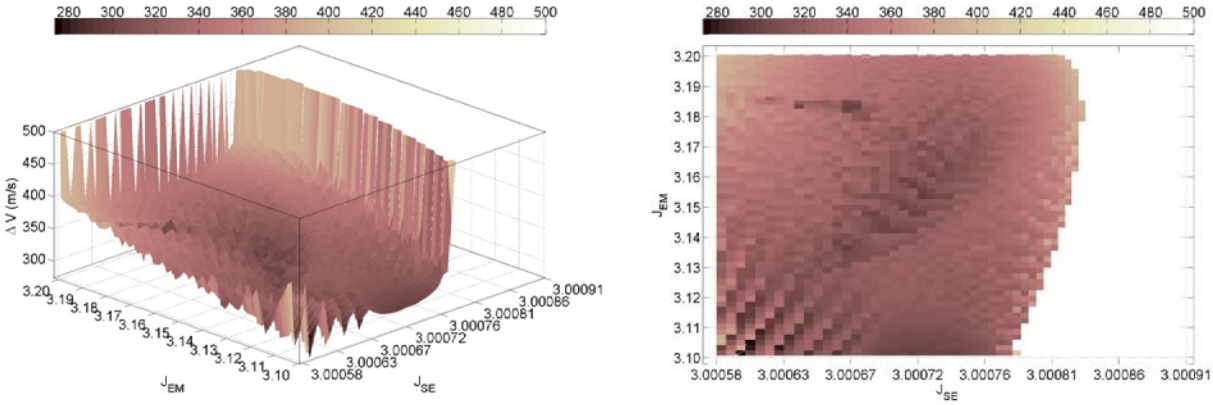

Fig. 8. 3D (left) and 2D (right) color maps of minimum ΔV for connections of type L^{SE}_2 - L^{EM}_1 as a function of the Jacobi constant of the two systems.

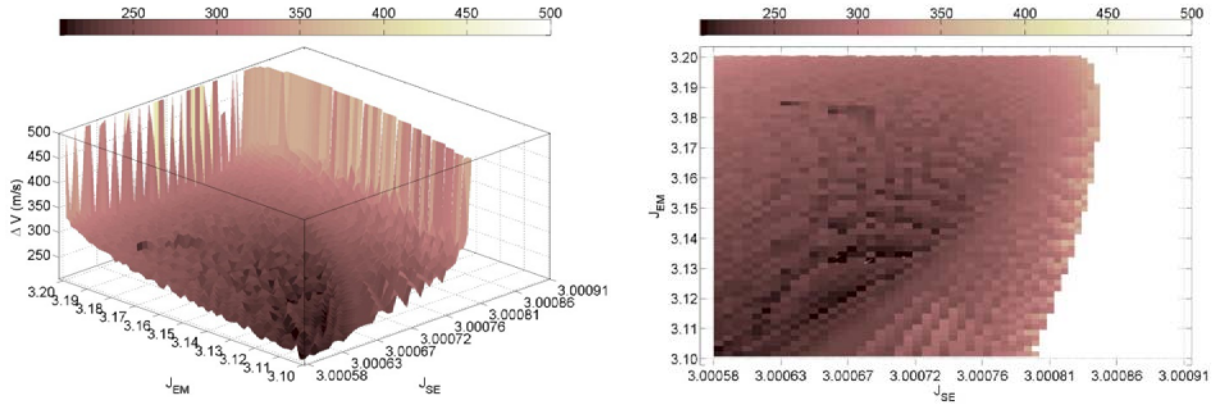

Fig. 9. 3D (left) and 2D (right) color maps of minimum ΔV for connections of type L^{SE}_1 - L^{EM}_1 as a function of the Jacobi constant of the two systems.

3. WSB REGIONS AROUND THE EARTH AND THE MOON

3.1 Osculating Keplerian orbits around the second primary

Let us consider a CR3BP composed by two primaries P_1 and P_2 of masses m_1 and m_2, respectively. Consider initial conditions corresponding to osculating Keplerian orbits around P_2 at $t=0$ in a sidereal (i.e., inertial) reference frame centered on P_2 and such that the lines of absides $l(\theta)$ of such ellipses form angles θ with the positive x-axis of the synodical barycentric frame of reference. Be r_2 the pericenter distance, assumed to be the starting point of the motion. If a, e and E_k respectively denote the semi-major axis, the eccentricity and the total mechanical energy of such an osculating ellipse, then well-known two-body formulas state that

$$r_2 = a\,(1 - e) \tag{2}$$

$$E_k = -\frac{\mu}{2a} \tag{3}$$

Under such circumstances, the initial sidereal velocity $\mathbf{v}$, which is perpendicular to the position at the pericenter $\mathbf{r_2}$, can have two opposite directions, thus producing either osculating retrograde orbits (in the following indicated as endowed with positive velocity), or osculating direct orbits (with negative velocity). Introducing the first primary, and transforming (rotation of angle θ and shift of origin from the second primary to the barycentre of the system) the given motion in the synodical barycentric reference frame of the resulting CR3BP, provides the following set of initial conditions:

$$\begin{aligned} x &= r_2\cos\theta - 1 + \mu, & \dot{x} &= (r_2 - v)\sin\theta, \\ y &= r_2\sin\theta, & \dot{y} &= (v - r_2)\cos\theta \end{aligned} \tag{4}$$

for positive velocity, and

$$\begin{aligned} x &= r_2\cos\theta - 1 + \mu, & \dot{x} &= (r_2 + v)\sin\theta, \\ y &= r_2\sin\theta, & \dot{y} &= -(r_2 + v)\cos\theta \end{aligned} \tag{5}$$

for negative velocity.

The expressions of the Jacobi constant J for the two cases are obtained by introducing Eqs. 4 and 5 into the definition

$$J = x^2 + y^2 + \frac{2(1-\mu)}{r_1} + \frac{2\mu}{r_2} + \mu(1-\mu) - \dot{x}^2 - \dot{y}^2. \tag{6}$$

Recalling that v depends on pericenter distance and eccentricity, i.e.,

$$v^2 = \mu\left(\frac{2}{r_2} - \frac{1}{a}\right) = \frac{\mu(1+e)}{r_2}, \tag{7}$$

one obtains:

$$J_{\pm} = 2\cos\theta(1-\mu)r_2 + \frac{\mu(1-e)}{r_2} + \frac{2(1-\mu)}{\sqrt{r_2{}^2 - 2r_2\cos\theta + 1}} + (1-\mu) \pm 2\sqrt{\mu(1+e)r_2}, \tag{8}$$

where + or - precede the last term for positive and negative initial sidereal velocity, respectively. Note that $J_{\pm}$ is a function of e, r_2 and θ. In particular, when $J_{\pm}$ is fixed and e and θ are given, Eq. (8) must be solved numerically for r_2. In the present study, the bisection method has been adopted in order to approximate the smallest (i.e., closest to the primary) positive real root. Note, however, that when put in polynomial form, Eq. 8 becomes a twelfth-degree equation in r_2 and all the roots of the associated polynomial can be numerically obtained via the method of Laguerre ([7]).

3.2 Stable and unstable motions

According to the algorithmic definition given in [1], the motion of the third body P_3 around P_2 is said to be stable if, after leaving $l(\theta)$, P_3 makes one full revolution about P_2 without having first revolved around P_1, and its orbit has negative Keplerian energy relative to P_2 on return at $l(\theta)$. Whenever such condition is violated, the corresponding initial condition is said to be unstable. This includes trajectories which collide with either primary. In this study the stability criterion has also been applied with more than one revolution and even non integer numbers n_R of revolutions around P_2. n_R can be viewed as a parameter of the problem and its values determine the instantaneous border of the stable region (i.e., the set of points in phase space of the CR3BP which represent initial conditions that satisfy the stability definition). In other words, the border of the stable region evolves with time, or better with n_R.

The analysis of the structure of a WSB region and the study of the dynamics of its points can be carried out in two alternative ways:

- Mode 1: fixing $e = \bar{e}$ and varying J: a grid of points is set up in phase space by varying the distance r_2 from P_2, and the angle θ within a two-dimensional grid; from each (r_2, θ) pair and for a given choice of the direction of the initial velocity vector in sidereal coordinates ($v>0$ or

$v<0$) the remaining relevant quantities are computed: the J of the trajectory (Eq. 8) and its initial conditions (Eqs. 4 or 5) in the CR3BP frame of reference.

- Mode 2: fixing $J = \bar{J}$ and varying e: a grid of points is set up in phase space by varying the eccentricity e and the angle θ within a two-dimensional grid; from each (e, θ) pair and for a given choice of the direction of the initial velocity vector in sidereal coordinates ($v>0$ or $v<0$), the remaining relevant quantities are computed: the distance r_2 from the second primary (solution of Eq. 8) and the initial conditions (Eqs. 4 or 5) in the CR3BP frame of reference. Note that the solution of Eq. 8 in r_2 may not exist in the interval between the minimum allowed distance r_{2min} from the second primary (i.e., typically its surface radius) and the maximum r_{2max} set by the size of the problem (typically $r_{2max} << 1$). In this investigation, the search has been limited to the smallest real solution of Eq. 8, found by bisection.

3.3 The Sun-Earth and the Earth-Moon systems

Results concerning mode 1 can be found in [4] and [8] for the Earth-Moon CR3BP and will not be presented again here. We shall rather deal with simulations of mode 2 because these allow to investigate trajectories that correspond to fixed values of the Jacobi constant in the two systems, as in the low-energy transfers.

Mode 2 simulations have been performed according to the parameters defined in Table 1. The unstable points of the WSB regions around the Earth have been computed up to n_R = 1.5 revolutions around the second primary and the stability/instability criterion has been applied every 0.5 revolutions (Δn_R =0.5). Table 2 gives, for each of the two directions of the initial sidereal velocity, the number n_U (in %) of unstable points as n_R increases, and the final number n_S of stable points left over at n_R = 1.5. In the following, we shall consider the border of the weak stability boundary region between n_R =1.0 and n_R =1.5 and the corresponding stable and unstable points (column 4 and 5 of Table 2). Fig. 10 shows the location of the unstable points in configuration space in the interval between 1.0 and 1.5 revolutions around the Earth.

Table 1. Grid of initial conditions for mode 2 ($J = \bar{J}$) for the SE CR3BP with $\bar{J}_{SE}$ = 3.000583. When not specified, units are meant as CR3BP normalized. The initial set of (θ,e) pairs (line three) produces, when the solution of the fifth-order equation in r_2 falls in the range [r_{2min}, r_{2max}], a set of points (last line) that constitute the fundamental database of initial conditions for WSB computations.

	SE, $v>0$	SE, $v<0$
θ	[0°, 360°[	[0°, 360°[
$\Delta\theta$	1°	1°
E	[0.0, 1.0[	[0.0, 1.0[
Δe	0.005	0.005
No. of pairs	72000	72000
[r_{2min}, r_{2max}]	[$5 \cdot 10^{-5}$, 0.8]	[$5 \cdot 10^{-5}$, 0.8]
No. of points	49768	71830

Table 2. Percentage of unstable points (n_U) for increasing number of revolutions around the second primary (columns 2 to 4), percentage of points which are still stable (n_S) after $n_R = 1.5$ revolutions, total initial number of points (n_T). Each row corresponds to a specific simulation type, i.e., each of the two opposite directions of the initial sidereal velocity, for constant $J = \bar{J}_{SE} = 3.00583$.

Sim. type	n_U (%)			n_S (%)	n_T
	$0 \le n_R \le 0.5$	$0.5 \le n_R \le 1.0$	$1.0 \le n_R \le 1.5$	$n_R = 1.5$	
SE, $v>0$	54.0	36.0	9.0	1.0	49768
SE, $v<0$	0.2	6.0	4.7	89.1	71830

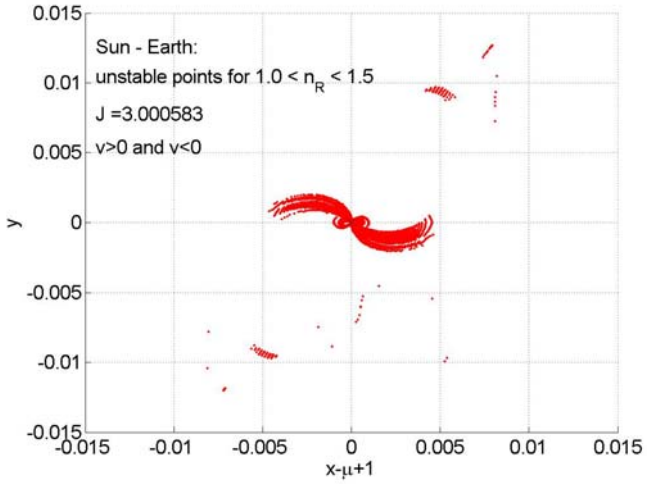

Fig. 10. Points which become unstable between 1.0 and 1.5 revolutions around P_2 for $\bar{J}_{SE} = 3.000583$ and for the two opposite signs of the initial sidereal velocity vector: x- and y-coordinates of the position in the synodical frame of reference with origin at P_2 (i.e., the Earth).

3.3 Earth WSB: capture around L_1 and L_2

The unstable points can be subdivided according to the resulting motion. To this purpose, and with the final aim of studying the points which get close to the collinear libration points L_1 and L_2, a capture criterion has been defined. It identifies the unstable points that approach L_1 or L_2 and stay in their vicinity for an appreciable time. The criterion here adopted consists in defining for each L_i (i=1,2) two circles (of radii r_{B1i} and r_{B2i}, i=1,2) centered on the second primary and three straight lines orthogonal to the x-axis (at x coordinates x_{ai}, x_{bi}, and x_{ci}, respectively), and two time parameters, namely t_{max} and τ: the former is the maximum allowed time interval for a capture to begin, the latter is the minimum capture duration. The capture region is the area enclosed by the two circles and the straight line through x_a and x_b. The capture criterion rejects all trajectories which for $0 \le t \le t_{max}$ do any of the following:

- enter and exit the region enclosed by the two circles, coming from P_2;
- cross the $x=x_{ci}$ line in the direction of increasing distance from P_2;
- exit the larger of the two circles;
- collide with one of the primaries.

On the contrary, points which spend a time $\Delta t \geq \tau$ inside the capture region and start such stay at $0 \leq t \leq t_{\max}$, are said to be captured in the vicinity of the given L_i. Fig.11 defines the capture geometry in the SE system. The capture criterion also discriminates among points which enter one or both capture regions without performing capture and identifies which region is visited first. In brief, seven types of unstable points can be distinguished: rejected points, captured points around L_1, captured points around L_2, points visiting the capture region ar ound L_1 only, points visiting the capture region of L_2 only, points visiting first the region around L_1 and then the region around L_2, points visiting first the region around L_2 and then the region around L_1. Fig. 12 shows some trajectories that get temporarily captured around L_1 and L_2.

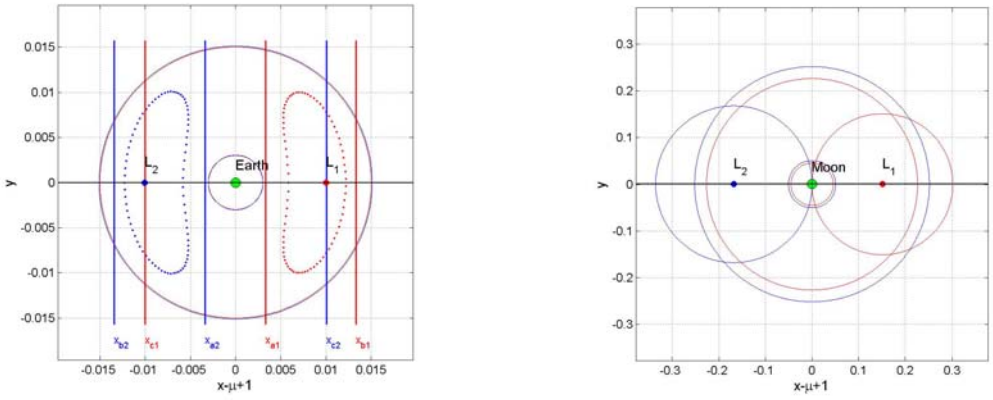

Fig. 11. Geometry of the capture regions around L_1 and L_2 for the Sun-Earth (left) and the Earth-Moon (right) systems. Also shown are the two planar Lyapunov orbits of the given energy.

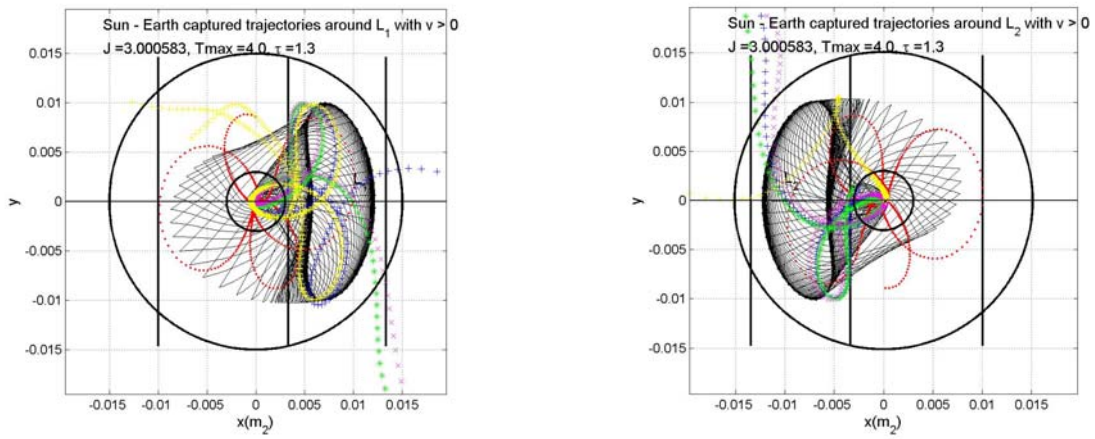

Fig. 12. Some trajectories belonging to the unstable subset of points of the WSB region around the Earth that get captured around L^{SE}_1 (left) and L^{SE}_2 (right), according to the criterion defined in the text. Also shown are the corresponding planar Lyapunov orbits and their stable manifolds.

With the aim of relating the invariant manifolds with the set of unstable points, Fig. 13 shows the points of the stable and unstable manifolds of L^{SE}_1 and L^{SE}_2 which satisfy the orthogonality condition

between the position vector and the velocity vector relative to the second primary (the Earth), in the and the points belonging to the WSB region of the Earth that become unstable between 1.0 and 1.5 revolutions around the Earth. The agreement between the two sets of points is good, thus suggesting that a dynamical relationship between them does exist.

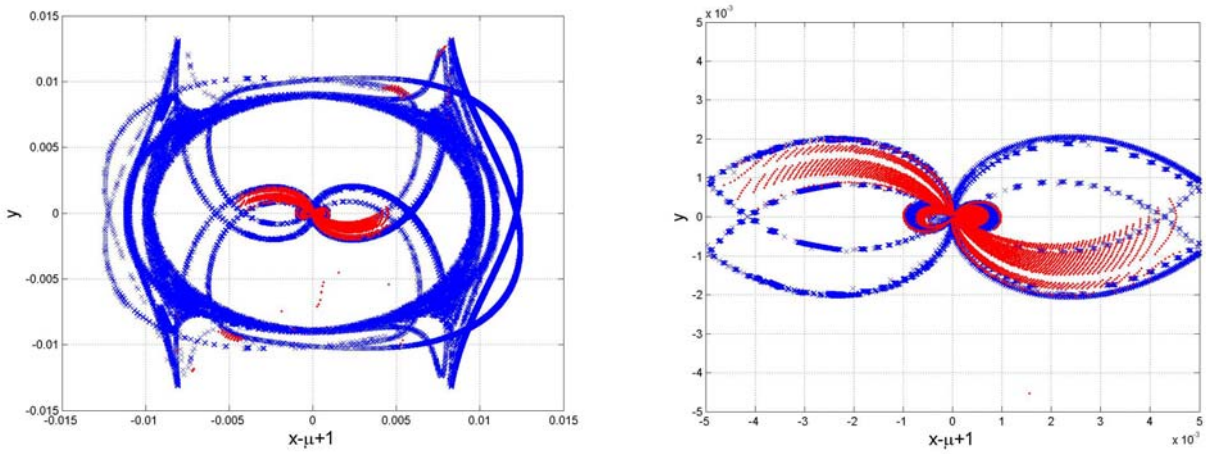

Fig. 13. Sun-Earth system: points (blue crosses) of the stable and unstable manifolds of the Lyapunov orbits around L^{SE}_1 and L^{SE}_2 with J_{SE}=3.000583 which satisfy the orthogonality condition and WSB points (red dots) that become unstable after 1.0 and before 1.5 revolutions around the Earth and have the same energy level as the manifolds. The left plot shows the complete picture, whereas the right plot is an enlarged view of the region around the Earth.

4. WSB TRAJECTORIES IN THE BICIRCULAR FOUR-BODY PROBLEM

The initial conditions corresponding to unstable points of the SE CR3BP with $J = \bar{J}_{SE} = 3.000583$ and $1.0 \leq n_R \leq 1.5$ that perform capture around L^{SE}_1 or L^{SE}_2 are integrated in the B4BP. Here, a second capture criterion is applied to check for subsequent capture around L^{EM}_1 or L^{EM}_2 (geometrically defined), with the aim at connecting the libration points of the two systems. This "second" capture at L^{EM}_j is said to occur when the third body stays more than 0.5 days in the region enclosed by two circles centered on the Moon and the circle centered on the corresponding libration point and radius equal to its distance from the Moon (See Fig. 11 b).

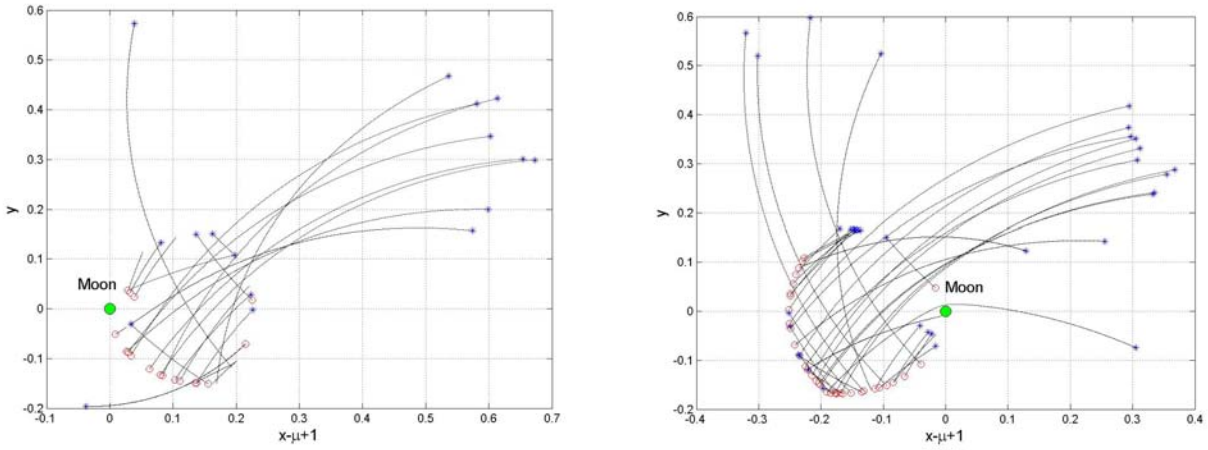

Fig. 14. Examples of trajectories that depart from the vicinity of the Earth, get captured around L^{SE}_1 or L^{SE}_2 and finally transit through the region of capture around L^{EM}_1 (left) or L^{EM}_2 (right). The red circles indicate the beginning of the capture, the blue asterisks the end of the numerical integration.

Our current simulations show that several trajectories which are initially captured around L^{SE}_1 or L^{SE}_2 pass through the second capture regions around L^{EM}_1 or L^{EM}_2 (Fig. 14), satisfying the capture criterion, but none of them gets into orbit around the Moon nor seems to be driven by stable manifolds associated to L^{EM}_1 or L^{EM}_2. This may be due to the need for varying the fundamental parameter linking the two systems, i.e., the initial relative orbital phase: the computation to which Fig. 13 refers has been made by assuming $\alpha_0 = 0$.

5. CONCLUSIONS

In this paper we have investigated the connection between the unstable points of the WSB regions with the low-energy transfers from the Earth to the Moon. The first part of the study consisted in an exploration of all the possible low-energy L^{SE}_i-L^{EM}_j connections between the Sun-Earth and the Earth-Moon CR3BPs. Such study is in course of refinement by considering the same transfers in the B4BP: a database containing the dynamical substitutes of the Lyapunov orbits and their invariant manifolds have been prepared and the exploration of the connections is being carried out.

The investigation concerning the relationship between the WSB regions of the Earth and the Moon needs to be refined as far as the variation of the initial relative orbital phase between the Sun-Earth and the Earth-Moon systems is concerned. Besides, more simulations with different values of the Jacobi constant in the Sun-Earth CR3BP will help verifying the hypothesis that the low-energy transfers from the Earth to the Moon are made by the points that leave the WSB region of the Earth and that perform the sequence of the two captures.

The computations performed in the CR3BP are based on the use of a Runge-Kutta 7-8 numerical integrator and the equations of motion are regularized in the vicinity of the primaries by means of the Levi-Civita method (see [9] and [2]). The simulations in the B4BP use a Taylor numerical integrator, instead, which is known to be more accurate when close approaches occur. Nevertheless, regularization will need to be implemented and this will be done either by considering some global regularization

method or a strategy involving the Levi-Civita method and the reduction from four to three bodies during close encounters.

ACKNOWLEDGMENTS E.Fantino and Y.Ren have been supported by the Marie Curie Actions Research and Training Network AstroNet. G. Gómez and J.J. Masdemont have been partially supported by the MCyT grants MTM2006-05849/Consolider and MTM2006-00478, respectively.

6. REFERENCES

[1] Belbruno E.A., *Capture Dynamics and Chaotic Motions in Celestial Mechanics: With Applications to the Construction of Low Energy Transfers*, Princeton University Press, Princeton, New Jersey, 2004.

[2] Stiefele E.L. and Scheifele G., *Linear and Regular Celestial Mechanics*, Springer-Verlag, 1971.

[3] Circi C. and Teofilatto P., *On the Dynamics of Weak Stability Boundary Lunar Transfers*, CELESTIAL MECHANICS AND DYNAMICAL ASTRONOMY, Vol. 79, 41-72, 2001.

[4] García F. and Gómez G., *A note on weak stability boundaries*, CELESTIAL MECHANICS AND DYNAMICAL ASTRONOMY, Vol. 97, 87-100, 2007.

[5] Koon W.S., et al., *Low energy Transfer to the Moon*, CELESTIAL MECHANICS AND DYNAMICAL ASTRONOMY, Vol. 81, 63-73, 2001.

[6] Miller J.K. and Belbruno E.A.**,** *A method for the construction of a lunar transfer trajectory using ballistic capture*, Proceedings of the 1st AAS/AIAA Annual Spaceflight Mechanics Meeting (A93-17901 05-13), 97-109, 1991.

[7] Press W.H., et al., *Numerical Recipes in FORTRAN 77: The Art of Scientific Computing*, Cambridge University Press, Cambridge, 1992.

[8] Romagnoli D. and Circi C., *Earth-Moon Weak Stability Boundaries in the restricted three and four body problem*, CELESTIAL MECHANICS AND DYNAMICAL ASTRONOMY, Vol. 103, 79-103, 2009.

[9] Szebehely V., *Theory of Orbits*, Academic Press, New York and London, 1967.